Alzheimer's
Research & Therapy

RESEARCH

Open Access

Rotation errors in path integration are associated with Alzheimer's disease tau pathology: a cross-sectional study

Lise Colmant[1,2,3*], Lisa Quenon[1,2], Lara Huyghe[1], Adrian Ivanoiu[1,2], Thomas Gérard[1,2], Renaud Lhommel[2], Pauline Coppens[1], Yasmine Salman[1], Vincent Malotaux[1,4], Laurence Dricot[1], Lukas Kunz[5], Nikolai Axmacher[6], Philippe Lefèvre[1,3] and Bernard Hanseeuw[1,2,4]

Abstract

Background Early Alzheimer's disease diagnosis is crucial for preventive therapy development. Standard neuropsychological evaluation does not identify clinically normal individuals with brain amyloidosis, the first stage of the pathology, defined as preclinical Alzheimer's disease. Spatial navigation assessment, in particular path integration, appears promising to detect preclinical symptoms, as the medial temporal lobe plays a key role in navigation and is the first cortical region affected by tau pathology.

Methods We have conducted a cross-sectional study. We related the path integration performance of 102 individuals without dementia, aged over 50, to amyloid and tau pathologies, measured using positron emission tomography. We included 75 clinically normal individuals (19 with brain amyloidosis, 56 without) and 27 individuals with mild cognitive impairment (18 with brain amyloidosis, 9 without). We fitted linear mixed models to predict the path integration performances according to amyloid status or tau pathology in the medial temporal lobal, adjusting for age, gender, cognitive status, education, and video game experience. We decomposed the error into rotation and distance errors.

Results We observed that clinically normal adults with brain amyloidosis (preclinical Alzheimer's disease) had spatial navigation deficits when relying only on self-motion cues. However, they were able to use a landmark to reduce their errors. Individuals with mild cognitive impairment had deficits in path integration that did not improve when a landmark was added in the environment. The amyloid status did not influence performance among individuals with mild cognitive impairment. Among all individuals, rotation, but not distance, errors increased with the level of tau pathology in the medial temporal lobe.

Conclusion Our results suggest that path integration performance in an environment without external cues allows identifying individuals with preclinical Alzheimer's disease, before overt episodic memory impairment is noticeable. Specifically, we demonstrated that poor angular estimation is an early cognitive marker of tau pathology, whereas distance estimation relates to older ages, not to Alzheimer's disease.

Trial registration Eudra-CT 2018–003473-94.

Keywords Spatial navigation, Path integration, Alzheimer's disease, Early diagnosis, Tau pathology

*Correspondence:
Lise Colmant
lise.colmant@uclouvain.be
Full list of author information is available at the end of the article

Background

Alzheimer's disease (AD) is characterized by the accumulation of amyloid beta (Aβ) plaques and tau aggregates in the brain [1]. This accumulation begins before the onset of cognitive impairment [2]. Amyloid deposits may be the earliest evidence of AD, the preclinical stage of which is defined by brain amyloidosis without cognitive impairment [3]. Although individuals with preclinical AD perform within normal ranges on standard neuropsychological tests, they are at risk of developing cognitive impairment [3, 4]. The development of highly sensitive cognitive tests to identify subtle impairment indicative of preclinical AD in the general population is thus critically important for screening and enrolling at-risk individuals in AD prevention trials.

Spatial navigation, in particular path integration, may be among the first cognitive abilities impaired in AD, from the preclinical stage [5–7]. Path integration is the ability to continuously keep track of and return to a previously visited location [8]. It is guided by information derived from self-motion (idiothetic) cues and landmarks (allothetic cues), when available. Path integration relies on neural computations in the medial temporal lobe (MTL), including the entorhinal cortex (EC) and the hippocampus (HC) [9]. It may be particularly supported by grid cells in the EC [10–13], which fire in a hexagonal pattern in response to self-motion cues [14]. When only self-motion cues are available, errors in path integration and grid cell firing tend to accumulate. These errors can be corrected by additional environmental features, which are processed in multiple brain regions, including the HC [15]. The HC contains place cells that fire in a particular position in space [16].

In AD, the MTL is among the first cortical regions to show tau pathology [17]. The spread of tau pathology within the MTL may impair grid-cell functioning and lead to path integration deficits in the early stages of AD [7, 18, 19]. Several studies have revealed path integration deficits in individuals at risk of AD development [20–22]. These path integration deficits would first occur when only self-motion cues are available [20, 21, 23], and would be corrected with the use of allothetic cues [23]. However, none of these studies involved the measurement of tau pathology in the human MTL. Mouse models of Alzheimer's disease have revealed grid cells impairment and path integration deficits before spatial cognition impairment [18, 19, 24], and a recent study showed that path integration errors were associated positively with the plasma p-tau181 level in humans [25]. The recent development of second-generation tau tracers used with positron emission tomography (PET) enables the imaging of tau aggregates in the human MTL and comparison of locoregional tau-PET signals with path integration performance. We made use of these new technological advances to compare tau accumulation with path integration behavior. Experimental paradigms of path integration enable the distinction between rotation and distance errors. Recent computational models of path integration suggest that rotation errors occur specifically in AD [26], whereas distance errors occur predominantly with age [21]. However, whether the neuropathology of AD impairs rotation and/or distance errors is unknown.

In this study, we investigated associations among visual path integration performance, Aβ, and tau-PET measures in individuals without dementia. The visual path integration task contained trials depending only on self-motion cues [pure path integration (PPI)] and trials in which an external landmark was added [landmark-supported path integration (LPI)]. We hypothesized that individuals with preclinical AD would have an isolated PPI deficit, as when amyloid accumulates in the brain, tauopathy begins to spread into the MTL, which could impair grid cells functioning, while other brain regions processing landmarks remain functional [27]. We expected that path integration deficits will be higher among patients with mild cognitive impairment (MCI) than among clinically normal (CN) individuals. Furthermore, we aimed to disentangle the impacts of Aβ and tau on the different processes underlying path integration in early AD. Specifically, we examined the impact of tau in the MTL on rotation versus distance errors, hypothesizing that rotation errors would be related to tau pathology whereas distance errors would be related to age.

Methods

Participants

We recruited adults aged > 50 years without dementia in Belgium, including participants from our previous study [21] and patients at the Memory Clinic of Saint-Luc University Hospital (UCLouvain, Belgium). Individuals with focal brain lesions, epileptic seizures, major depression, psychiatric conditions, and alcohol or drug abuse were excluded. We have conducted a cross-sectional study based on data available in the cohort study. In our cross-sectional study, eligible individuals had a Mini-Mental State Examination (MMSE) score ≥ 24/30 [28], normal or corrected-to-normal vision, and no recent illness or change in medical treatment during the previous 3 months. Recruitment and examinations were conducted between June 2019 and May 2024. Two hundred and twelve individuals have been recruited in the cohort study including tau-PET. We recruited for the path integration task from this cross-sectional study, excluding 60 individuals because they had dementia, 4 individuals because they died shortly after the tau-PET, 25 because they did not realize all examinations (MRI, amyloid

measurement, tau-PET, standard neuropsychological examinations), 18 individuals because they refused to carry out the path integration task, and 3 individuals because they tried the path integration task but failed and stopped during the training. This resulted in 102 individuals performing all the exams.

Participants performed the "Apple Game" visual path integration task [20, 21, 29], a [^{18}F]-MK-6240 tau-PET examination [30, 31], a structural brain magnetic resonance imaging (MRI), an apolipoprotein E (*APOE*) genotyping, a standard neuropsychological evaluation, and the measurement of brain amyloidosis via PET or cerebrospinal fluid (CSF) analysis. Clinically normal participants were genetically pre-selected to be included in the study, as that 50% of them were *APOE* ε4 carriers. This proportion matched the one observed in the patients attending the Memory clinic and allowed to enrich the sample in individuals with preclinical AD.

Ethics approval declaration

This study was conducted in accordance with the Declaration of Helsinki and approved by the institution's Ethics Committee (UCL-2016–121). All participants provided written informed consent (Trial registration: Eudra-CT 2018–003473-94).

APOE genotyping

DNA was extracted from participants' blood samples, analyzed to detect the *APOE* polymorphisms, and assigned two of the following alleles: ε2, ε3, or ε4. The *APOE* ε4 allele is a major risk factor of AD [32]. We classified participants as ε4 carriers (ε3ε4, ε4ε4, and ε2ε4) or ε4 noncarriers (ε2ε2, ε2ε3, and ε3ε3).

Neuropsychological evaluation

The standard neuropsychological evaluation involved the assessment of four cognitive domains: memory (French version of the free and cued selective reminding test [33]), language [Lexis naming test, category fluency test (animals), and letter fluency test ("P") [34]], executive function (Luria's graphic sequences and trail making test [35]), and visuospatial function (clock drawing test [36] and the praxis part of the Consortium to Establish a Registry for Alzheimer's Disease battery [37]). *Z*-scores were computed for each cognitive domain. Scores below −1.50 standard deviation (SD) of an independent sample (composed of 32 CN individuals who remained cognitively stable over 8 years) were considered to indicate impairment [38]. MCI was defined as an MMSE score ≥ 24/30 and impairment in at least one cognitive domain.

MRI

Participants underwent three-dimensional (3D) T1-weighted MRI examination at Saint-Luc University Hospital (UCLouvain, Belgium) using a 3 T head scanner (Signa™ Premier; General Electric Company, USA) equipped with a 48-channel coil. The dataset encompassing the whole brain was selected to acquire detailed (1 mm^3 scale) anatomical information with a magnetization prepared rapid gradient echo sequence (inversion time = 900 ms, repetition time = 2188.16 ms, echo time = 2.96 ms, flip angle = 8°, field of view = 256×256 mm^2, matrix size = 256×256, number of slices = 156, slice thickness = 1 mm, no gap, total scan time = 5 min 36 s). A three-dimensional T2-weighted sequence was also acquired using the same scanner.

The T1 MR images were segmented with FreeSurfer (version 7.2) into cortical [39] and subcortical [40] regions. The T2 sequences were used to improve segmentation. All MRI segmentations were verified visually and corrected as needed. This process resulted in the segmentation of the EC, HC, and estimated total intracranial volume (eTIV). Averages of the left and right EC and HC volumes were calculated.

[^{18}F]-MK-6240 tau-PET

Tau-PET recordings were realized with [^{18}F]-MK-6240 (Lantheus, Bedford, MA, USA). Ninety minutes after the intravenous administration of [^{18}F]-MK-6240 (target activity = 185 ± 5 MBq), a 30-min list-mode PET/computed tomography (CT) examination was performed using a Philips Vereos digital scanner (Philips Healthcare, Amsterdam, The Netherlands). Images were reconstructed using the manufacturer's algorithm, which includes attenuation, scatter, and decay corrections and time-of-flight information. Point spread functions were calculated and 1 mm reslicing was performed using the manufacturer's algorithm to obtain better resolution recovery. We used averaged 6×5 min standardized uptake values (SUVs).

Tau-PET images were co-registered on the T1 MR images using the PetSurfer pipeline [41, 42]. We computed the SUV ratio (SUVr) of an MTL meta-region, composed of the EC and HC, using the cerebellum gray matter as a reference. The MTL SUVr was used for analyses, due to the strong correlation of the EC and HC SUVrs (Pearson correlation coefficient, $r = 0.92$). We did not distinguish tau in the right and left MTL for the same reason ($r = 0.95$).

Two trained nuclear physicians (R.L. and T.G.) determined a visual stage (Tau+ vs. Tau-) for every tau-PET fused with a 3D T1 MRI for precise anatomical reference. The Braak stage was used to determine this status. Based

on previous work by Schöll and colleagues on Braak staging applied to brain imaging [43], regions were determined and grouped into categories. Tau- corresponds to Braak 0 (not a single positive region); Tau+ corresponds to Braak I-II-III-IV-V-VI (Tau signal at least in the MTL) [30].

Determination of amyloid status

Participants' amyloid status was determined by amyloid-PET ($n=88$), or lumbar puncture with CSF analysis ($n=14$). Participants with abnormal amyloid values (CSF Aβ42 level < 437 pg/ml [44], or amyloid-PET Centiloid value ≥ 26 [45]) were classified as amyloid positive (Aβ+). Other participants were classified as amyloid negative (Aβ-).

Amyloid-PET

Two amyloid-PET radiotracers were used in this study: [^{18}F]-flutemetamol (GE Healthcare, Chicago, IL, USA; $n=68$) and [^{11}C]-Pittsburg Compound B ([^{11}C]-PiB; $n=20$). A Centiloid value was computed for both radiotracers using the PNEURO software (version 4.1; PMOD LLC Technologies, Zurich, Switzerland) [45, 46].

CSF analysis

Aβ42 in the CSF was measured using the Lumipulse® assay (G β-Amyloid 1–42, ref. 230,336) in the Biology Laboratory of Saint-Luc University Hospital (UCLouvain, Belgium).

Classification of participants

Participants were classified as CN Aβ-, CN Aβ+ (preclinical AD), MCI Aβ-, or MCI Aβ+. We compared participants' age, education (in years), video game experience (in hours/week of game play), MMSE, and tau in the MTL among groups using ANOVA. Post-hoc pairwise *t*-tests, corrected for multiple comparisons using the Holms method, were conducted when differences among groups were detected. We compared participants' gender and *APOE* ε4 carriage using chi-squared tests.

Experimental task

Participants performed the Apple Game visual path integration task [20, 21, 29], implemented via Unreal Engine (version 4.11; Epic Games). The game was displayed on a 15-inch high-definition screen, and participants moved in a virtual environment using a joystick. The joystick allowed them to move forward, turn left, or turn right, such that movement direction was identical to heading direction. The linear and rotation speeds were not constant and depended on the inclination of the joystick. Participants' positions were sampled at 5 Hz.

The game environment was an endless grassy field with a blue sky rendered at infinity. Each players arrived at a start location in the field. In the start phase,

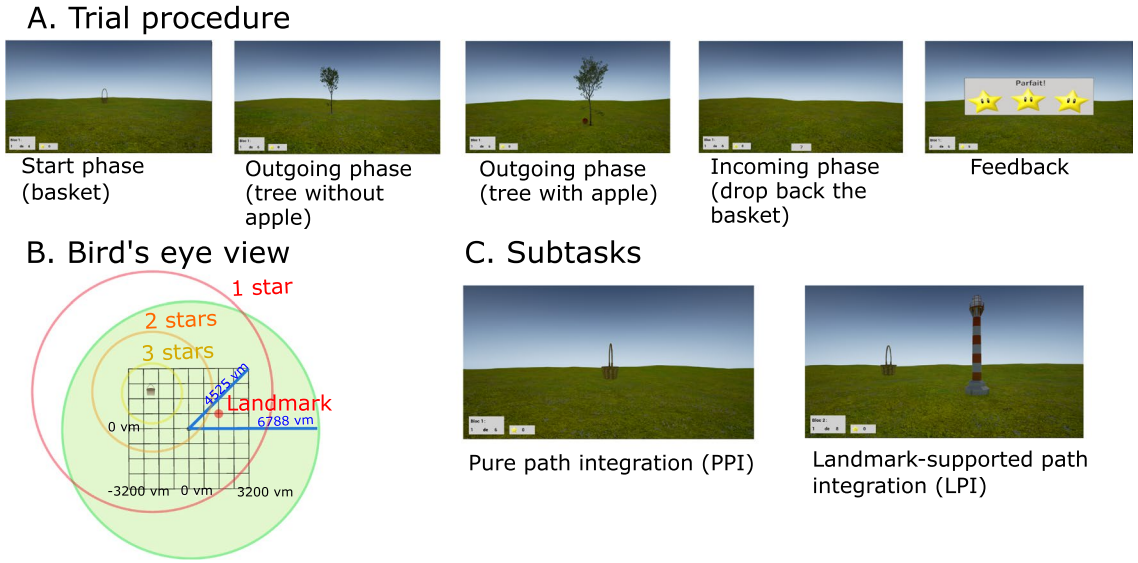

Fig. 1 Experimental paradigm. **A** Trial procedure: players pick up an empty basket (start phase), find an apple under a tree (outgoing phase), and return the basket to its remembered location (incoming phase). They then receive feedback (as stars) according to the distance between the correct and remembered basket location. **B** Bird's eye view of the virtual environment. Baskets and trees were positioned randomly in an 8 × 8 grid (3200 × 3200 vm). Under the landmark-supported path integration condition, the landmark (a lighthouse) was located at x = 1600 vm and y = 800 vm. **C** The task consisted of two subtasks depending on the presence or absence of supportive spatial cues. The pure path integration (PPI) subtask contained no external cues, whereas the landmark-supported path integration (LPI) subtask contained a landmark

they looked for and collected an empty basket (Fig. 1A). Then, a tree appeared in the environment, with or without an apple at its base. In both cases, participants were asked to walk toward the tree. When they reached it, the tree disappeared. If there had been no apple at the base of the first tree, a second tree with an apple appeared. Participants walked from tree to tree (outgoing phase; Fig. 1A) until reaching the tree with the apple. After collecting the apple, they were asked to return, as directly as possible, to the remembered original basket location (incoming phase; Fig. 1A) and return (drop) the basket. The players then received feedback on their performance via zero to three stars. The number of stars depended on the Euclidean distance between the original and drop basket locations [< 1600 virtual meters (vm; the game environment unit given by Unreal Engine [20]) for three stars, < 3200 vm for two stars, < 6400 vm for one star; Fig. 1B].

The incoming phase had a time limit of 30 s; all other phases were self-paced. The mean time of the incoming phase was 16.42 s (SD = 6.9 s). When a participant did not return the basket within the time limit, their final position was recorded as drop location (6.2% of all trials).

The locations of baskets and trees were distributed randomly on an invisible grid of 8 × 8 squares (bin edge length = 800 vm; Fig. 1B). The grid was surrounded by an invisible circular area with a radius of 1.5 × grid half diagonal (6788 vm). Participants could not move outside of this circular area, and their speed decreased linearly to zero when their distance from the center of the area exceeded 5656 vm. This action was implemented to ensure that participants did not navigate too far away from the relevant part of the infinite environment.

The task was implemented as two environmental subtasks, defined by the absence or presence of supportive spatial cues (Fig. 1C). In the "pure path integration" subtask (PPI), the environment did not contain any landmarks. In the "landmark-supported path integration" subtask (LPI), a landmark, represented by a lighthouse, which looked the same from every angle, was present in the virtual environment.

The paradigm was subdivided in five blocks of eight trials (four PPI and four LPI subtasks in pseudo-random order) each. The first block was a training block, and data from it were not analyzed. Each subtask consisted of two trials with one tree, and two trials with two trees, in pseudo-random order. In trials with one tree, the apple was at the base of the first tree. In trials with two trees, the first tree was a distractor (increasing the difficulty of path integration), and the apple was at the base of the second tree. Participants started the first trial in each block at the center of the virtual environment. In subsequent trials, their start locations corresponded to their final locations in the previous trial. Between each trial, a black screen was displayed for 5 s.

A subsample of participants ($n = 33$) performed previous versions of the task. A paradigm of five blocks with six trials (three PPI and three LPI subtasks) each was used for 30 participants [21]. The first block remained a training block. The subtasks consisted of one, two, and three trees (with the apple at the base of the final tree in all cases) in pseudo-random order. Three participants performed the original version of the Apple Game, which consists of trials with one to five trees and three subtasks (PPI, LPI, and boundary-supported path integration) [20]. For these subsamples, we analyzed only data from PPI and LPI subtasks implemented with one or two trees. We used a random effect in our models to account for the difference in paradigm versions.

Performance parameters

Participants' performance was quantified using the drop error (Fig. 2A), which is the Euclidean distance between the original and drop basket locations. We decomposed the drop error into distance and rotation errors. The distance error is the absolute difference between the incoming distance (distance from the apple collection location to the correct basket location) and the response distance (distance from the apple collection location to the drop location; Fig. 2B). The rotation error (0–180°) is the angle between the drop location, the apple collection location, and the correct basket location (Fig. 2C). When the response distance was 0 vm, the rotation error was not defined as the apple collection location corresponded to the drop location (27.4% of trials without distractor tree, and for 26.8% of trials with one distractor tree). In most trials with 0 vm as response distance, participants still rotated before dropping the basket (4.7% of trials had 0 vm as response distance and no rotation after reaching the apple). When the response distance was 0 vm and no rotation was performed after reaching the apple, participants could have misunderstood the task, as they seemed "catching" the apple and not bringing back the basket to its original location. We removed these trials (0 vm as response distance and no rotation after reaching the apple) from the analyses.

Statistical analysis

We extracted behavioral data from logfiles using MATLAB (version 2020a; The MathWorks Inc.). The statistical analyses were conducted with R (version 4.3.2; R Core Team) using the lmerTest (version 3.1.3) [47] and emmeans (1.8.9) [48] packages. We reported results for the condition with no distractor tree; results for the condition with a distractor tree, particularly difficult for older participants [21], are provided in Additional File 1.

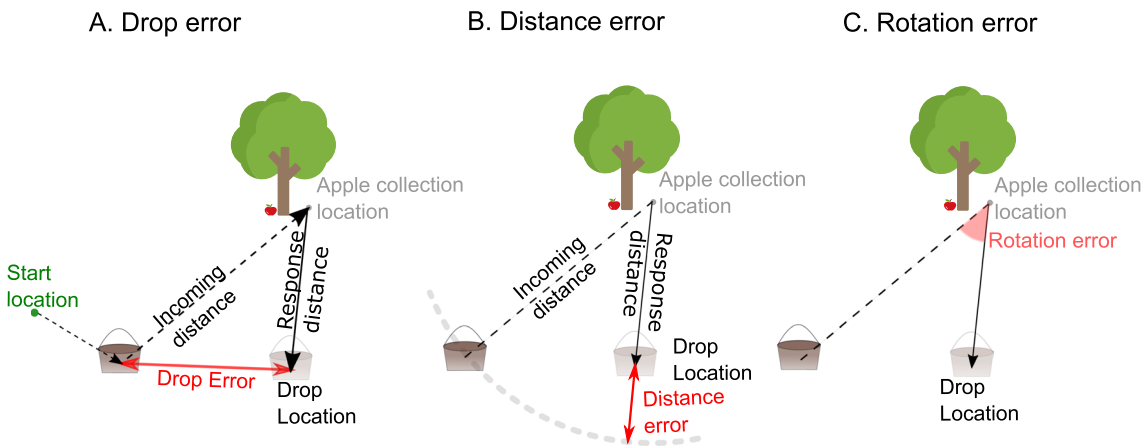

Fig. 2 Metrics used to evaluate visual path integration task performances. **A** Drop error. The drop error is the Euclidean distance between the correct and drop basket locations. The incoming distance is the distance between the apple collection location and the correct basket location. The response distance is the distance between the apple collection location and the drop location. **B** Distance error. The distance error is the absolute difference between the incoming and response distances. **C** Rotation error. The rotation error is the angle between the basket, the apple collection location, and the drop location

We analyzed participants' spatial navigation performance using linear mixed models. The participant and paradigm version were allocated as random factors in all models. All distance variables were divided by 1000 for expression as virtual kilometers. Participant age, gender, and education were covariates in all models. Video game experience was introduced as a covariate in models including Apple Game data. We report all significant effects. Statistical tests were two-tailed and significance level was set to $\alpha = 0.05$. *P*-values for main effects were calculated using Satterthwaite's degree of freedom and lmerTest [47]. Post-hoc analyses were conducted to examine the effects of variables within interactions, using estimated marginal means, with covariates set to the average (emmeans function) [48].

Assessment of the effect of amyloid status on path integration

We modeled the drop error with the amyloid status (Aβ + vs. Aβ-), cognitive status (CN vs. MCI), subtask (PPI vs. with LPI), and their interactions as predictors:

$$\begin{aligned} Drop\ error = {} & \beta_0 + \beta_{0i} + \beta_{0j} + \beta_1 A\beta + \beta_2 cognitive\ status + \beta_3 subtask \\ & + \beta_4 age + \beta_5 APOE + \beta_6 gender + \beta_7 education \\ & + \beta_8 video\ game + \beta_{12} A\beta * cognitive\ status + \beta_{13} A\beta * subtask \\ & + \beta_{23} cognitive\ status * subtask + \beta_{123} A\beta * cognitive\ status * subtask + \beta_9 dt \end{aligned} \quad (1)$$

where β_{0i} is a random intercept per participant, β_{0j} is a random intercept per paradigm version, dt is the mean time interval between the apple game and the other exams (amyloid measurement, neuropsychological evaluation, and tau-PET). As the variable effects could vary with task difficulty (number of trees), we constructed separate models for the two difficulty levels. We performed post-hoc analysis to determine whether the drop error differed between subtasks for CN or MCI individuals, whether the drop error differed between amyloid status for a given cognitive status and subtask, and whether the drop error differed between subtasks for a given cognitive and amyloid statuses [48].

We also tested the three-way interaction between *APOE* status, amyloid status, and cognitive status. The three-way interaction was not significant. The drop error was not different between *APOE* ε4 carriers and ε4 non-carriers among CN Aβ-, CN Aβ+, MCI Aβ-, and MCI Aβ + individuals.

To confirm the effect found among individuals with preclinical AD was not related to an older age, we performed a subsample analysis. We included all CN Aβ + individuals ($n = 19$) and added the 19 older CN Aβ- individuals. We fitted the Eq. 1b on this subsample:

$$\begin{aligned} Drop\ error = {} & \beta_0 + \beta_{0i} + \beta_{0j} + \beta_1 A\beta + \beta_3 subtask + \beta_4 age \\ & + \beta_5 APOE + \beta_6 gender + \beta_7 education \\ & + \beta_8 video\ game + \beta_{13} A\beta * subtask + \beta_9 dt \end{aligned} \quad (1b)$$

Assessment of the effect of amyloid status on composite cognitive scores

We modeled the different cognitive *z*-scores using linear models with the amyloid status, cognitive status, and their interactions as predictors:

$$Zscore = \beta_0 + \beta_1 A\beta + \beta_2 cognitive\ status + \beta_3 age + \beta_4 gender + \beta_5 education + \beta_{12} A\beta * cognitive\ status \quad (2)$$

We performed post-hoc analysis to evaluate the effect of the amyloid status for each cognitive status [48].

Assessment of the effect of amyloid status on MRI measures

We modeled the EC and HC volumes using linear models with the amyloid status, cognitive status, and their interactions as predictors, the eTIV was added as covariates:

$$Volume = \beta_0 + \beta_1 A\beta + \beta_2 cognitive\ status + \beta_3 eTIV + \beta_4 age + \beta_5 gender + \beta_6 education + \beta_{12} A\beta * cognitive\ status \quad (3)$$

We performed post-hoc analysis to evaluate the effect of the amyloid status on the HC and EC volumes for each cognitive status [48].

Assessment of the effect of tau pathology

We analyzed the effect of tau in the MTL on the drop error and its components (rotation and distance errors). As the MTL tau SUVr distribution was not normal, we log-transformed the data. Linear mixed models were computed to estimate errors according to tau in the MTL. We added the following covariates: amyloid status, cognitive status, *APOE* ε4 carriage, video game experience, and mean time interval between the apple game and the other exams (amyloid measurement, neuropsychological evaluation, and tau-PET).

$$Error = \beta_0 + \beta_{0i} + \beta_{0j} + \beta_1 \ln(tauMTL) + \beta_2 A\beta + \beta_3 cognitive\ status + \beta_4 subtask + \beta_5 age + \beta_6 gender + \beta_7 APOE + \beta_8 education + \beta_9 video\ game + \beta_{10} dt \quad (4)$$

where β_{0i} is a random intercept per participant and β_{0j} is a random intercept per paradigm version, dt is the mean time interval between the apple game and the other exams (amyloid measurement, neuropsychological evaluation, and tau-PET). We computed separate models for both difficulty levels. To determine whether the tau signal improves the model, we performed a model comparison between the Eq. 4 and the same equation without the tau signal as predictor.

As the impact of tau pathology could vary according to the presence or absence of the landmark, we also tested the interaction between the subtask (PPI vs. LPI) and tau signal. As the interaction was never significant, the interaction was not added in the final model.

To examine whether the effect of tau on path integration was specific to regions involved in path integration (i.e., the MTL), we repeated the models using the frontal pole region instead of the MTL. We choose the frontal pole region as a control region because it is not involved in path integration and is not affected by tauopathy early in AD development. As the SUVr distribution for the frontal pole region did not follow a normal distribution, we log-transformed the data.

Assessment of the effect of composite cognitive scores on path integration performance

The effects of composite cognitive *z*-scores on the errors were analyzed using the following linear mixed model equation:

$$Error = \beta_0 + \beta_{0i} + \beta_{0j} + \beta_1 z\ memory + \beta_2 z\ visuospatial + \beta_3 z\ language + \beta_4 z\ executive + \beta_5 age + \beta_6 gender + \beta_7 education + \beta_8 video\ game + \beta_9 dt \quad (5)$$

where β_{0i} is a random intercept per participant, β_{0j} is a random intercept per paradigm version, and dt is the mean time interval between the apple game and the other exams (amyloid measurement, neuropsychological evaluation, and tau-PET). We constructed separate models for both difficulty levels and subtasks.

Assessment of the effects of MRI measures on path integration performance

The effects of MRI measures on the errors were analyzed. We focused on the EC and HC volumes, as tau pathology was quantified in a meta-region including these two regions. The EC and HC volumes followed a normal distribution, as assessed visually with a qqplot. The eTIV were added as covariates:

$$Error = \beta_0 + \beta_{0i} + \beta_{0j} + \beta_1 EC\ volume + \beta_2 HC\ volume + \beta_3 eTIV + \beta_4 age + \beta_5 gender + \beta_6 cognitive\ status + \beta_7 education + \beta_8 video\ game + \beta_9 dt \quad (6)$$

where β_{0i} is a random intercept per participant and β_{0j} is a random intercept per paradigm version, and dt is the mean time interval between the apple game and the other exams (amyloid measurement, neuropsychological evaluation, and tau-PET).. We constructed separate models for both difficulty levels and subtasks. Then, we applied the same equation with the addiction of the amyloid status as a covariate.

Results

Classification of participants

Participants were assigned to four groups: CN Aβ- ($n=56$), CN Aβ+(preclinical AD; $n=19$), MCI Aβ- ($n=9$), and MCI Aβ+($n=18$; Table 1). As expected,

Table 1 Classification of participants. Education is expressed in years of studies. Video game experience is expressed as hours/week of video game play. Tau in the MTL is the tau SUVr for a meta-region composed of the EC and HC, with the cerebellum gray matter serving as a reference region. Participants were enriched in *APOE* ε4 carriers to reach 50% of carriers. [a]ANOVA, [b]chi-squared test. SD: standard deviation. MTL: medial temporal lobe

	CN Aβ-	CN Aβ+	MCI Aβ-	MCI Aβ+	*p*
n	56	19	9	18	
Age: mean (SD)	67.1 (7.9)	73.0 (6.5)	71.1 (8.0)	71.7 (8.8)	0.02[a]
MMSE: mean (SD)	28.6 (1.2)	28.3 (1.1)	27.6 (1.8)	26.4 (2.1)	0.0024[a]
Gender: M/F	26/30	8/11	5/4	9/9	0.97[b]
APOE ε4 carriers: n (%)	23 (41%)	13 (68%)	5 (56%)	10 (56%)	0.19[b]
Education: mean (SD)	16.3 (2.6)	16.7 (3.0)	17.3 (4.2)	16.1 (3.9)	0.85[a]
Video game experience: mean (SD)	0.91 (2.91)	1.63 (3.37)	0.55 (1.13)	0.89 (2.17)	0.66[a]
Tau in the MTL: mean (SD)	0.84 (0.21)	1.11 (0.29)	0.92 (0.12)	1.60 (0.55)	$7.2\ 10^{-6}$ [a]
Amyloid measurement: PET/CSF	54/2	18/1	8/1	8/10	$3.8\ 10^{-7}$[b]

individuals in the CN Aβ- group were younger than those in the CN Aβ+group ($P=0.031$). The MMSE score was lower in the MCI Aβ+groups than in the CN Aβ- and CN Aβ+groups ($P<0.0001$ and $P=0.0008$, respectively). Participant gender, *APOE* ε4 carriage, education, and video game experience did not differ significantly among groups. The MTL tau SUVr was higher in the CN Aβ+groups than in the CN Aβ- group ($P=0.004$), and higher in the MCI Aβ+group than in the CN Aβ-, CN Aβ+, and MCI Aβ- groups (all $P<0.0001$). Of course, patients MCI Aβ+benefitted more often from CSF analysis for clinical reasons.

Individuals with MCI had path integration deficits that were not corrected by landmark use

Cognitive status was associated with the drop error (Eq. 1, $t_{181}=2.16$, $P=0.032$; Fig. 3; Additional Table 1), indicating that MCI individuals performed worse than CN individuals on the path integration task. The errors were also larger without landmark than with landmark ($t_{1210}=2.47$, $P=0.014$), and were positively associated with age ($t_{86}=3.83$, $P=0.0002$). There was no effect of the *APOE* status. Post-hoc analysis revealed that individuals with MCI performed significantly worse than CN individuals in LPI ($t_{173}=3.07$, $P=0.0025$), but not

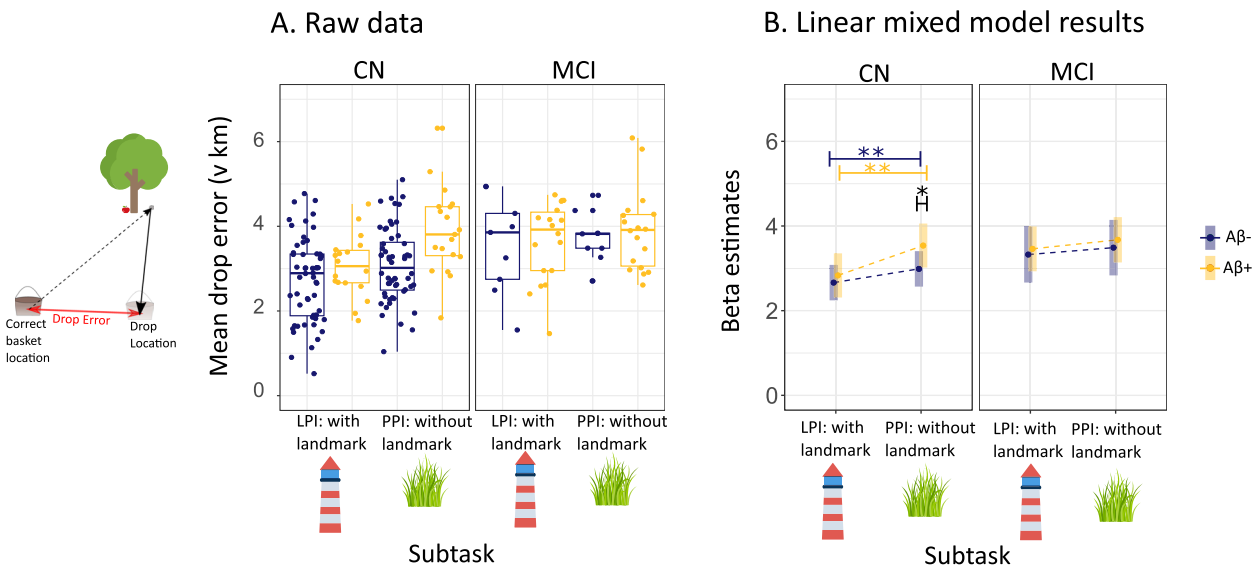

Fig. 3 Path integration performance according to cognitive and amyloid statuses. **A** Raw data without distractor tree. Each point represents the mean drop error of a participant. **B** Linear mixed model results (Eq. 1), the y-axis represents beta estimates of the drop error according to the subtask, amyloid status, and cognitive status. Error bars represent 95% confidence intervals. CN: clinically normal, MCI: mild cognitive impairment, LPI: landmark-supported path integration, PPI: pure path integration. *$0.01<P<0.05$, **$0.001<P<0.01$

in PPI (Additional Table 1). Aβ status did not modify the PPI or LPI performance of individuals with MCI (Fig. 3). Furthermore, landmark use did not decrease these individuals' error relative to PPI (Fig. 3). These results suggest that individuals with MCI have spatial navigation difficulties and do not benefit from landmark use.

CN Aβ + individuals had a path integration deficit that was corrected by landmark use

Post-hoc comparisons showed that the drop error in PPI was larger among CN Aβ + than CN Aβ- individuals ($t_{168} = 2.29$, $P = 0.023$; Fig. 3, Additional Table 1). LPI performance did not differ according to Aβ status in both CN groups. The error decreased by adding the landmark in both CN groups (Aβ-: $t_{1202} = -2.47$, $P = 0.014$; Aβ + : $t_{1203} = -3.15$, $P = 0.0017$; Additional Table 1). Thus, landmark use benefitted CN individuals, regardless of Aβ status, in contrast to the results for individuals with MCI. CN Aβ + individuals performed similarly to CN Aβ- individuals in the standard neuropsychological evaluation (Eq. 2; Additional Table 2; Additional Fig. 1) and had comparable EC and HC volumes (Eq. 3; Additional Table 3), suggesting that the path integration task disclosed more subtle neurocognitive deficits than revealed by standard episodic memory tests or structural MRI.

To confirm that the higher error observed in PPI among individuals with preclinical AD was not related to an older age, we compared the errors of the 19 individuals with preclinical AD to the errors of the 19 older CN Aβ- individuals. The mean age of CN Aβ + individuals was 73.0 years old, and the mean age of the CN Aβ- subgroup was 75.8 years old. The age difference between the two groups was not significantly different (p = 0.13). In this subsample, we confirmed that CN Aβ + individuals had a higher drop error than Aβ- individuals in PPI (Eq. 1b, $t_{53} = 2.73$, $P = 0.0085$, effect size = 0.43), and not in LPI ($t_{53} = 0.64$, $P = 0.52$, effect size = 0.10).

Tau pathology in the MTL was associated with the drop error

We hypothesized that the path integration deficit observed in CN Aβ + individuals was due to incipient tau pathology in the MTL. Indeed, we observed more tau accumulation in the MTL in CN Aβ + than in CN Aβ- individuals ($t_{97} = 3.69$, $P = 0.0004$, Table 1). The drop error was associated with the increasing level of tau in the MTL (Eq. 4, $t_{185} = 2.19$, $P = 0.029$, Additional Table 4). We then separated the drop error into its two components, rotation, and distance errors, to identify the exact effect of tau on path integration.

Rotation error was associated with tau pathology in the MTL and distance error with age

Using the same model predicting errors with tau in the MTL (Eq. 4), we observed that participants' rotation error was associated positively with tau accumulation in the MTL ($t_{79} = 3.56$, $P = 0.0006$; Fig. 4, Table 2). We tested the interaction between tau in the MTL and the subtask, which was not significant suggesting that tau in the MTL affects similarly the angle estimation with and without landmark. In contrast, the distance error was not associated with tau in the MTL (Fig. 4, Table 2). The rotation error increased with age ($t_{78} = 2.71$, $P = 0.008$). The age

Table 2 Effects of tau in the MTL, amyloid status, cognitive status, subtask, age, gender, APOE status, education, video game experience, and mean time interval between Apple Game and other exams (amyloid measurement, tau-PET, neuropsychological evaluation) on the rotation and distance errors (Eq. 4). PPI: pure path integration, LPI: landmark-supported path integration, df: degrees of freedom, CI: confidence interval, CN: clinically normal, MCI: mild cognitive impairment, M: male, F: female, dt: examination time interval. *$0.01 < p < 0.05$. **$0.01 < p < 0.001$. ***$p < 0.001$

	Rotation error				Distance error			
	Estimate (95% CI)	**df**	***t***	***P***	**Estimate (95% CI)**	**df**	***t***	***P***
Intercept	1.92 (−44.55 – 48.34)	82	0.077	0.94	−0.31 (−2.06 – 1.47)	90	−0.32	0.75
ln(Tau in MTL)	33.2 (15.99 – 50.49)	79	3.56	0.00064***	0.27 (−0.38 – 0.93)	88	0.78	0.44
Amyloid status (Aβ + vs. Aβ-)	−9.99 (−21.23 – 1.48)	79	−1.63	0.11	0.41 (−0.02 – 0.84)	89	1.77	0.08
Cognitive status (MCI vs. CN)	10.03 (−1.44 – 21.33)	84	1.63	0.11	0.21 (−0.21 – 0.63)	89	0.92	0.36
Subtask (PPI vs. LPI)	12.68 (7.11 – 18.39)	916	4.40	$1.2\ 10^{-5}$ ***	0.20 (0.05 – 0.35)	1207	2.62	0.009**
Age	0.84 (0.26 – 1.41)	78	2.71	0.008**	0.04 (0.02 – 0.06)	89	3.37	0.0011**
Gender (M vs. F)	−4.91 (−13.80 – 4.17)	79	−1.01	0.32	−0.27 (−0.61 – 0.07)	91	−1.48	0.14
APOE (ε4 carrier vs. noncarrier)	3.50 (−5.17 – 12.27)	81	0.74	0.46	0.08(−0.25 – 0.41)	90	0.46	0.65
Education	0.05 (−1.44 – 1.54)	85	0.06	0.95	−0.04 (−0.10 – 0.012)	88	−1.43	0.16
Video game experience	0.41 (−1.15 – 1.96)	78	0.49	0.63	−0.04 (−0.11 – 0.02)	89	−1.30	0.20
dt	−1.83 (−8.11 – 4.61)	71	−0.53	0.60	−0.04 (−0.29 – 0.21)	87	−0.28	0.78

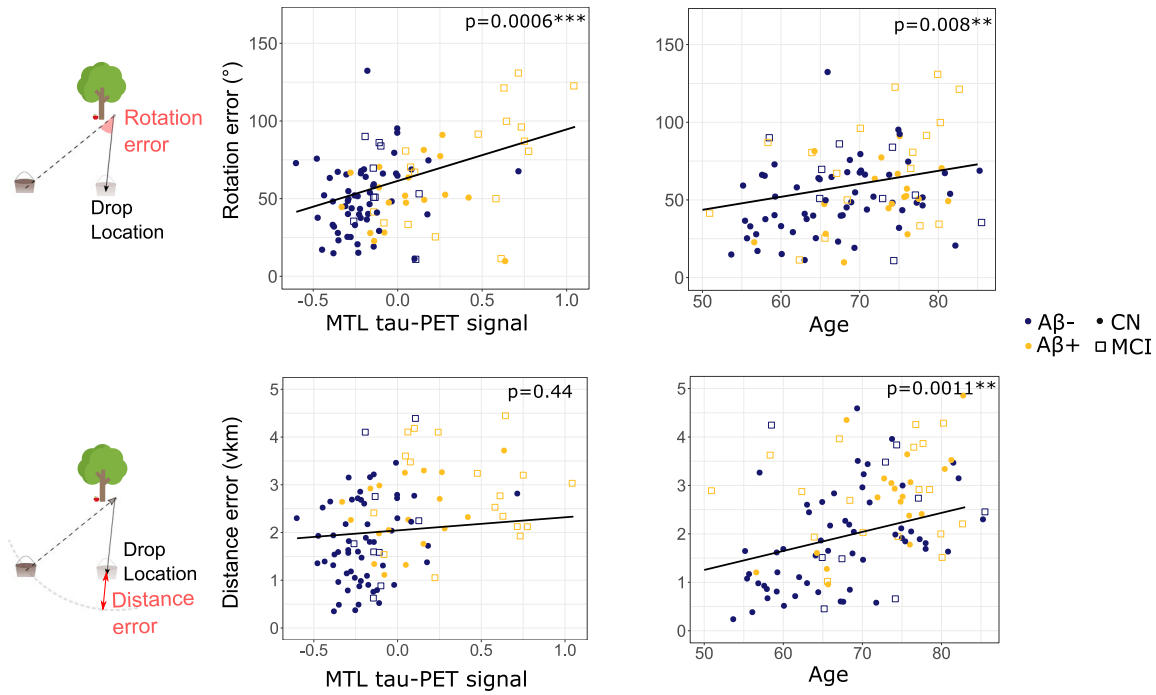

Fig. 4 Tau in the MTL was associated with the rotation error, not with the distance error. Dots represent mean errors of participants. Lines represent the effects of tau in corresponding subtasks from linear mixed models (Eq. 4). MTL tau-PET signals correspond to the natural logarithms of MTL tau SUVr (i.e., a tau-PET signal of 1 corresponds to an SUVr of 2.718). PPI: pure path integration, LPI: landmark-supported path integration, CN: clinically normal, MCI: mild cognitive impairment. *$0.01 < P < 0.05$; ** $0.001 < P < 0.01$; *** $P < 0.001$

was also associated with the distance error ($t_{89} = 3.37$, $P = 0.0011$; Fig. 4, Table 2). As tau and Aβ were adjusted for, these results indicate that age-related effects on distance estimation are attributable to a mechanism other than AD pathology.

The model comparison confirmed that adding tau signal as predictor (Eq. 4) improved the model for the drop error ($P = 0.013$) and the rotation error ($P = 0.00024$). When tau signal was not in the model, the cognitive status was associated with the rotation error (higher rotation error for MCI compared to CN individuals, $t_{87} = 2.85$, $P = 0.005$) and the drop error ($t_{88} = 2.73$, $P = 0.007$). However, adding tau signal in the model (Table 2) led to a non-significant effect of cognitive status on the rotation error. This suggests that the higher error of MCI individuals is explained by higher tau levels in their MTL.

The *APOE* genotype and amyloid status did not affect path integration

The model accounting for tau pathology revealed that participants' *APOE* status was not associated with their path integration performance under any subtasks (Eq. 4; Additional Table 4, Table 2). The amyloid status was not associated with the rotation error (Table 2), it trended to affect the distance error, but this effect was not significant ($t_{89} = 1.77$, $P = 0.08$; Table 2). Other covariates (cognitive status, gender, education, and video game experience) were not significant in any model.

The effect of tau pathology on the rotation error was observed specifically in the temporal lobe

To test whether the effect of tau on path integration was specific to regions involved in path integration, we reran the models using the frontal pole region instead of the MTL (Eq. 4). We found that tau in the frontal pole region was not related to path integration errors in any subtask, indicating that the effects of tau pathology on the path integration task were restricted to regions presumably involved in path integration computations.

Assessment between path integration and neuropsychological performances

We investigated whether composite cognitive scores reflecting episodic memory, language, visuospatial, and executive functions were associated with path integration performance (Eq. 5). For PPI, larger rotation errors were associated with lower visuospatial *z*-scores ($t_{77} = -2.56$, $P = 0.01$), and not with the other cognitive domain *z*-scores (Additional Table 5). For PPI, the drop and distance errors did not correlate with any *z*-score.

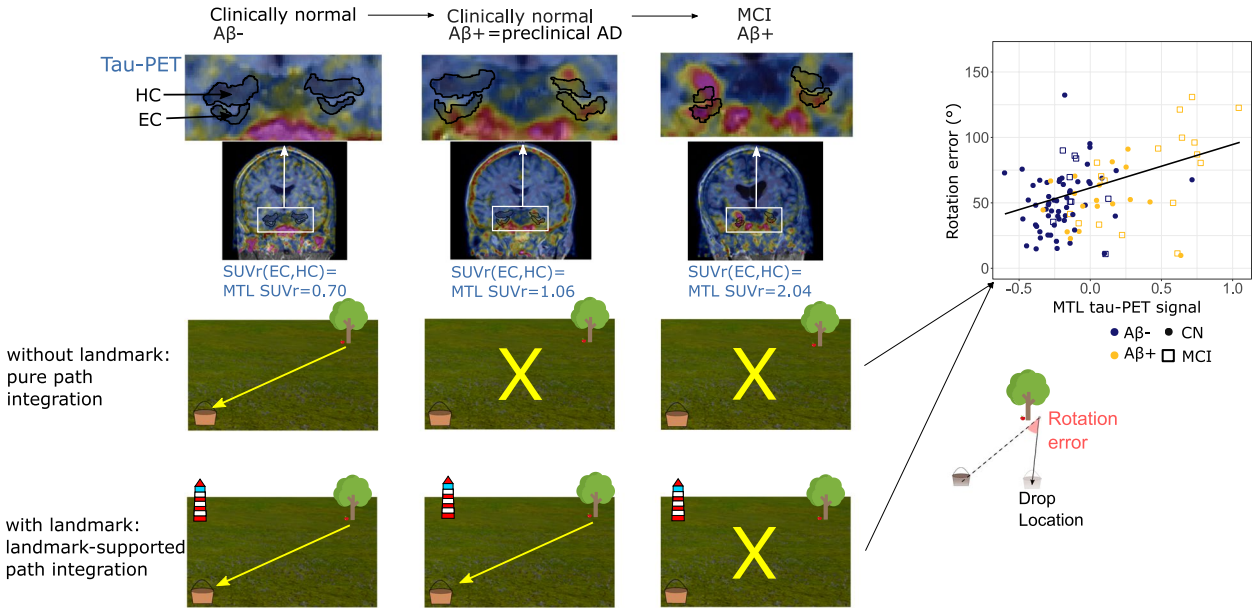

Fig. 5 Illustration of the associations among cognitive status, AD neuropathology, and path integration performance. Left: Clinically normal amyloid negative (Aβ-) individuals have no tau deposit, as the MTL SUVr is low. They can return to the goal location under pure and landmark-supported path integration conditions. Middle Left: Individuals with preclinical AD are clinically normal and amyloid positive (Aβ+), and have some tau accumulation in the MTL. They showed deficits in pure path integration, but can use the landmark to decrease their error. Middle Right: As AD progresses, individuals develop mild cognitive impairment (MCI) and have difficulties with pure and landmark-supported path integration. Right: Tau in the MTL is related to the rotation, but not distance, error. Dots represent mean errors of participants. Lines represent the effects of tau in corresponding subtasks from linear mixed models (Eq. 4)

For LPI, larger drop errors were associated with lower episodic memory *z*-scores ($t_{81}=-2.36$, $P=0.02$; Additional Table 5). Specifically, poorer episodic memory was associated with distance errors ($t_{86}=-2.03$, $P=0.04$). Larger distance errors were also associated with lower executive function *z*-scores ($t_{85}=-2.60$, $P=0.01$). The language *z*-score was not associated with any path integration metric.

Thus, PPI rotation error was associated with visuospatial abilities, whereas LPI distance error was related to episodic memory and executive functions.

Landmark processing was related to the HC volume

We examined whether the EC and HC volumes were associated with path integration performance (Eq. 6). The volumes were not associated with PPI performance (Additional Table 6). Smaller HC volumes were associated with larger drop errors in LPI ($t_{91}=-2.10$, $P=0.004$; Additional Table 6). This effect tended to disappear after adjustment for amyloid pathology ($t_{91}=-1.98$, $P=0.05$).

Discussion

The identification of the early stage of AD, before the onset of irreversible cognitive symptoms, is crucial for the development of preventive therapies. Individuals with the preclinical stage of AD cannot be identified with standard neuropsychological evaluation, as by definition they perform within normal ranges. In this study, we investigated a spatial navigation task, which highlighted a pure path integration deficit in individuals with preclinical AD (CN Aβ+) relative to CN individuals without AD neuropathology (CN Aβ-; Fig. 5). Individuals with preclinical AD seem able to use the landmark in the task to improve their path integration performance, as their LPI performance did not differ from that of CN Aβ- individuals. Navigation difficulties increase as cognitive impairment progresses, as reflected by the inability of patients with MCI to use the landmark to reduce their navigation task error in this study. The PPI deficit was not related to episodic memory performance, of to the EC or HC volumes, but depended on the visuospatial ability. The task used in this study, which assessed participants' ability to return to a goal location after visiting an intermediate location, shows promise for the identification of early cognitive symptoms of the disease and seems targeting the visuo-spatial domain, a cognitive domain infrequently investigated in AD studies. The potential contribution of MTL to spatial memory and the visual inspection of the environment is an area under investigation.

Previous studies showed that path integration is affected in mild AD dementia and in prodromal AD [6, 49]. In this study, we showed that patients with preclinical

AD already have a path integration deficit, specifically in an environment without external cues. We did not find any difference between the performance of MCI Aβ + and MCI Aβ- individuals. This is inconsistent with a previous study showing that patients with prodromal AD exhibited higher path integration errors than non-AD MCI patients [6]. One potential explanation for this result is that the task studied in this paper is a purely visual path integration task (task performed on a computer screen), whereas Howett et al. used an immersive virtual reality task [6]. The purely visual path integration task could be more challenging and leading to a ceiling effect among MCI individuals. This is reinforced by a study showing that older individuals performed disproportionately worse when navigating on a desktop environment compared to in an immersive virtual reality condition [50].

In this study, we confirmed that individuals with preclinical AD had incipient tau pathology in the MTL detectable using tau-PET. We showed that the path integration rotation error was associated with tau in the MTL (Fig. 4). The effect of the amyloid status was not significant in models adjusted for tau, suggesting that path integration performance was not related to amyloid status per se, but to tau pathology in the MTL. This finding is consistent with the view that tau pathology in AD is linked more directly to cognitive deficits than amyloidosis [51, 52]. Thus, rotation error in path integration could be a cognitive marker of tau in the MTL.

Our observations are consistent with previous demonstrations of pure path integration deficits in the absence of external cues in CN individuals at risk of AD development [20–22]. We further demonstrated that PPI performance was decreased in individuals with preclinical AD, and was not associated with other AD risk factors, such as *APOE* ε4 carriage when AD neuropathology was taken into account. Path integration deficits in early AD have been found in mouse models developing of brain amyloidosis [23, 53] and tauopathy [18, 24]. Ying and colleagues reported that idiothetic navigation becomes unreliable in early AD due to the disruption of grid cell coding, leading to the reduced integration of self-motion cues [23]. On the other hand, they showed that allothetic cues reshaped the spatial map in the EC in early AD. Altogether, these findings and ours suggest the presence of a deficit in grid cell functioning, which could be underpinned by EC activity dysfunction in the preclinical stage of AD [7]. This notion is also supported by the fact that EC atrophy mediates the association between the CSF p-tau181 level and spatial navigation in CN adults [54]. The absence of an LPI deficit in individuals with preclinical AD suggests that grid cells can still be stabilized by external cues in this early stage of the disease.

We demonstrated that tau in the MTL correlated specifically with the rotation error, and not with the distance error. Similar associations have been observed in patients with AD relative to controls [49] and in computational models of path integration in AD [26]. Of note, patients with right temporal lobectomy also displayed specific rotation errors during path integration task performance [55]. Thus, distance estimation may rely on brain regions outside of the temporal lobe. A functional MRI study demonstrated that poorer angular estimation is associated with the reduction of grid-like representations in midlife adults at risk of AD [22]. However, the pathological mechanism responsible for this angular deficit has not been elucidated. Further tau-PET and functional MRI studies are needed to demonstrate the association among tau in the MTL, grid-like representations in the EC, and rotation error.

We hypothesized that the effect of tau in the MTL on the rotation error is related to grid cells impairments due to tau pathology in the EC. However, no consensus on the role of grid cells in rotation versus translation in path integration has been established. Some findings suggest that grid cells act as vector-coding cells, playing roles in both rotation and translation [11, 56]. Alternatively, it has been suggested that grid cells code for translational path integration [27, 57], and that head direction cells (HDCs) are more relevant for angular path integration [57]. Our study does not allow to distinguish whether rotation error is related to grid cells or HDCs impairment, as some HDCs are localized in the EC. Furthermore, HDCs provide direct input to grid cells [58], making it impossible with current resolution of PET to distinguish between their respective contributions in human studies.

We observed that rotation and distance errors depended on age, highlighting the importance of controlling such a task for age. Unlike the rotation error, distance error did not depend on tau in the MTL. This deficit in distance estimation in older individuals has been reported previously [59], and we observed it in a larger group of participants who did not undergo tau-PET imaging [21]. It remains controversial, as one study revealed no significant effect of age on a distance reproduction task performance [60] and another study showed increased distance and rotation errors with age [61]. The interpretation of age effects in these studies is particularly difficult, as these effects are likely mixed with those of preclinical AD pathology, which is common in older individuals, and was not specifically examined in those studies. Interesting hypotheses beyond the scope of the current study, such as age-related reductions in sensory [62] and optic flow [63] processing resulting in noisy self-motion inputs, have been proposed.

The effect of tau in the MTL on rotation error observed in this study was not due to MTL atrophy, as the EC and HC volumes were not significantly associated with the PPI rotation error. We observed that HC atrophy was related to increased LPI drop errors. This finding is consistent with the role of the HC in the processing of external cues [64], and with our observation that landmark processing depends on episodic memory. It is also in line with the classical cognitive map theory [65], in which the HC is proposed to be the neural substrate of allothetic spatial information. Previous studies showed that the path integration errors were associated with the EC volume [6, 54]. We did not find this association in our study possibly because a smaller sample size (Coughlan et al. included 1875 clinically normal individuals [54]) or because we included less MCI individuals which may drive the EC volume effect (Howett et al. included 45 MCI individuals [6]). Previous studies have shown tau-PET changes precede volume changes in preclinical AD [66].

The task studied, moving to the goal location then to a single target and returning, is not a triangle completion task, as the task did not involve multiple directional changes. It could be considered as simplest path integration task. We tested a triangle completion task (adding a distractor tree), but this task was too difficult for participants older than 50 [21]. The drop error in trials with a distractor tree was not related to age, cognitive status, amyloid status, nor tau in the MTL in trials, confirming the task was too difficult for the population studied.

This study has several limitations. First, we included only participants aged > 50 years, which prevented us from examining the evolution of path integration performance across the entire lifespan. Second, we used a visual path integration task, in which participants did not use vestibular or proprioceptive information. Optic flow is particularly critical for this task, and little is known about the impact of preclinical AD pathology on optic flow processing. Third, the current spatial resolution of PET imaging does not allow for the distinction of signals in different MTL subregions (as the postero-medial EC, antero-lateral EC, or hippocampal subfields). Tau in the EC was strongly correlated with tau in the HC, preventing the distinction of the effects of these regions. Future work should address these challenges, and disentangle the contributions of volumetric measurements in these regions to path integration performances. Next, the relatively small sample of individuals with preclinical AD ($n = 18$) prevented the investigation of the effect of tau between tau negative and tau positive individuals in this subgroup (8 CN Aβ + T- and 10 CN Aβ + T + individuals). Finally, although promising for detecting individuals with preclinical AD, this task is not ready for clinical use. The task takes a long time to be completed (the mean duration was 30 min, excluding the explanation of the task, the training, and possible breaks during the test). Creating a simpler and shorter version of the task, for example containing 3 trials with no distractor tree (most informative trials) and 1 trial with one distractor tree in both conditions, could be valuable for the future. Before clinical implementation, future research work using shorter versions in larger samples should be conducted to confirm our observations.

Conclusions

In conclusion, we showed that individuals with preclinical AD had a specific deficit in pure path integration, when they had to navigate without external cues. When a landmark was available, individuals with preclinical AD were able to use it to improve their path integration performance. Navigation difficulties increase as cognitive impairment progresses, patients with MCI had difficulties to navigate with and without landmark. Furthermore, we observed that the path integration rotation error was associated with tau in the MTL, not with the amyloid status. Thus, rotation error in path integration could be a cognitive marker of tau in the MTL. The path integration task studied is promising to detect individuals with preclinical AD and/or brain tauopathy with a non-invasive and poorly expensive test.

Abbreviations

Aβ	Amyloid
Aβ +	Amyloid positive
Aβ-	Amyloid negative
AD	Alzheimer's disease
APOE	Apolipoprotein E
CI	Confidence interval
CN	Clinically normal
CSF	Cerebrospinal fluid
CT	Computed tomography
Df	Degrees of freedom
EC	Entorhinal cortex
eTIV	Estimated total intracranial volume
HC	Hippocampus
HDCs	Head direction cells
LPI	Landmark-supported path integration
MCI	Mild cognitive impairment
MMSE	Mini-Mental State Examination
MRI	Magnetic resonance imaging
MTL	Medial temporal lobe
PET	Positron emission tomography
PIB	Pittsburg Compound B
PPI	Pure path integration
SD	Standard deviation
SUV	Standardized uptake values
SUVr	Standardized uptake value ratio
Vm	Virtual meters

Supplementary Information

The online version contains supplementary material available at https://doi.org/10.1186/s13195-025-01679-w.

Additional file 1. Results with one distractor tree, neuropsychological evaluation: raw data, raw data of the rotation and distance errors.

Additional file 2: Additional Table 1 Effects of the cognitive status, amyloid status, age, gender, and *APOE* status on the drop error and contrasts from Eq. 1.

Additional file 3: Additional Table 2 Effects of the amyloid status, cognitive status, age, gender, and education on *z*-scores obtained by standard neuropsychological evaluation (Eq. 2).

Additional file 4: Additional Table 3 Effects of the amyloid status, cognitive status, eTIV, age, gender, and education on the EC and HC volumes (Eq. 3).

Additional file 5: Additional Table 4 Effects of tau in the MTL, amyloid status, cognitive status, subtask, age, gender, *APOE* status, education, and video game experience on the drop error (Eq. 4).

Additional file 6: Additional Table 5: Effects of composites cognitive z-scores on errors in PPI and LPI (Eq. 5)

Additional file 7: Additional Table 6: Effects of the EC and HC volumes on errors in PPI and LPI (Eq. 6).

Acknowledgements
We thank all participants and the Stichting Alzheimer Onderzoek for their help with this study.

Authors' contributions
L.C.: conceptualization, methodology, data analyses, visualization, investigation, writing - original draft. L.Q.: investigation. L.H.: investigation. A.I.: writing - review and editing. T.G.: investigation, formal analysis. R.L.: investigation, formal analysis. P.C.: investigation. Y.S.: investigation. V.M.: investigation. L.D.: conceptualization, writing - review and editing. L.K.: software, writing - review and editing. N.A.: software, writing - review and editing. P.L.: writing - review and editing, supervision. B.H.: writing - review and editing, supervision. All authors reveiwed the manuscript.

Funding
The Belgian Fund for Scientific Research (FNRS) provided grants for the personnel conducting this research (L.C.: no. ASP40001844, L.H.: no. ASP40016560). BJH acknowledges support from the FNRS (grant no. CCL40010417), the FRFS-WELBIO (grant no. 40010035), and the SOA-FRA. Fonds De La Recherche Scientifique—FNRS,ASP40001844,ASP40016560,FRIA40014635,CCL40010417,Stichting Alzheimer Onderzoek,Belgium,Walloon excellence in life sciences and biotechnology,40010035

Data availability
The datasets generated during the current study are available at https://doi.org/10.5281/zenodo.13805574.

Declarations

Ethics approval and consent to participate
This study was conducted in accordance with the Declaration of Helsinki and approved by the institution's Ethics Committee (UCL-2016–121). All participants provided written informed consent.

Consent for publication
Not applicable.

Competing interests
The authors declare no competing interests.

Author details
[1]Institute of Neuroscience, NEUR, UCLouvain, Avenue Mounier 53/B1.53.05, Brussels 1200, Belgium. [2]Department of Neurology, Cliniques Universitaires Saint-Luc, Brussels 1200, Belgium. [3]Institute of Information and Communication Technologies, Electronics and Applied Mathematics, UCLouvain, Louvain-La-Neuve 1348, Belgium. [4]Massachusetts General Hospital, Harvard Medical School, Boston, MA 02114, USA. [5]Department of Epileptology, University Hospital Bonn, Bonn 53127, Germany. [6]Department of Neuropsychology, Institute of Cognitive Neuroscience, Faculty of Psychology, Ruhr University Bochum, Bochum 44780, Germany.

Received: 24 October 2024 Accepted: 17 January 2025
Published online: 01 February 2025

References

1. Hyman BT, Phelps CH, Beach TG, Bigio EH, Cairns NJ, Carrillo MC, et al. National Institute on Aging–Alzheimer's Association guidelines for the neuropathologic assessment of Alzheimer's disease. Alzheimer's & Dementia. 2012;8:1–13.
2. Jack CR, Bennett DA, Blennow K, Carrillo MC, Dunn B, Haeberlein SB, et al. NIA-AA Research Framework: Toward a biological definition of Alzheimer's disease. Alzheimer's & Dementia. 2018;14:535–62.
3. Sperling RA, Aisen PS, Beckett LA, Bennett DA, Craft S, Fagan AM, et al. Toward defining the preclinical stages of Alzheimer's disease: Recommendations from the National Institute on Aging-Alzheimer's Association workgroups on diagnostic guidelines for Alzheimer's disease. Alzheimer's & Dementia. 2011;7:280–92.
4. Ossenkoppele R, Pichet Binette A, Groot C, Smith R, Strandberg O, Palmqvist S, et al. Amyloid and tau PET-positive cognitively unimpaired individuals are at high risk for future cognitive decline. Nat Med. 2022;28:2381–7.
5. Coughlan G, Laczó J, Hort J, Minihane A-M, Hornberger M. Spatial navigation deficits — overlooked cognitive marker for preclinical Alzheimer disease? Nat Rev Neurol. 2018;14:496–506.
6. Howett D, Castegnaro A, Krzywicka K, Hagman J, Marchment D, Henson R, et al. Differentiation of mild cognitive impairment using an entorhinal cortex-based test of virtual reality navigation. Brain. 2019;142:1751–66.
7. Igarashi KM. Entorhinal cortex dysfunction in Alzheimer's disease. Trends in Neurosciences. 2023;46(2):124–36 S0166223622002375.
8. Etienne AS, Jeffery KJ. Path integration in mammals. Hippocampus. 2004;14:180–92.
9. McNaughton BL, Battaglia FP, Jensen O, Moser EI, Moser M-B. Path integration and the neural basis of the "cognitive map." Nat Rev Neurosci. 2006;7:663–78.
10. Banino A, Barry C, Uria B, Blundell C, Lillicrap T, Mirowski P, et al. Vector-based navigation using grid-like representations in artificial agents. Nature. 2018;557:429–33.
11. Bush D, Barry C, Manson D, Burgess N. Using Grid Cells for Navigation. Neuron. 2015;87:507–20.
12. Gil M, Ancau M, Schlesiger MI, Neitz A, Allen K, De Marco RJ, et al. Impaired path integration in mice with disrupted grid cell firing. Nat Neurosci. 2018;21:81–91.
13. Jacobs J, Weidemann CT, Miller JF, Solway A, Burke JF, Wei X-X, et al. Direct recordings of grid-like neuronal activity in human spatial navigation. Nat Neurosci. 2013;16:1188–90.
14. Hafting T, Fyhn M, Molden S, Moser M-B, Moser EI. Microstructure of a spatial map in the entorhinal cortex. Nature. 2005;436:801–6.
15. Hardcastle K, Ganguli S, Giocomo LM. Environmental Boundaries as an Error Correction Mechanism for Grid Cells. Neuron. 2015;86:827–39.
16. O'Keefe J, Dostrovsky J. The hippocampus as a spatial map. Preliminary evidence from unit activity in the freely-moving rat. Brain Research. 1971;34:171–5.
17. Braak H, Braak E. Neuropathological stageing of Alzheimer-related changes. Acta Neuropathol. 1991;82:239–59.
18. Fu H, Rodriguez GA, Herman M, Emrani S, Nahmani E, Barrett G, et al. Tau Pathology Induces Excitatory Neuron Loss, Grid Cell Dysfunction, and Spatial Memory Deficits Reminiscent of Early Alzheimer's Disease. Neuron. 2017;93:533-541.e5.
19. Ridler T, Witton J, Phillips KG, Randall AD, Brown JT. Impaired speed encoding and grid cell periodicity in a mouse model of tauopathy. eLife. 2020;9:e59045.

20. Bierbrauer A, Kunz L, Gomes CA, Luhmann M, Deuker L, Getzmann S, et al. Unmasking selective path integration deficits in Alzheimer's disease risk carriers. Sci Adv. 2020;6:eaba1394.
21. Colmant L, Bierbrauer A, Bellaali Y, Kunz L, Van Dongen J, Sleegers K, et al. Dissociating effects of aging and genetic risk of sporadic Alzheimer's disease on path integration. Neurobiol Aging. 2023;131:170–81.
22. Newton C, Pope M, Rua C, Henson R, Ji Z, Burgess N, et al. Path integration selectively predicts midlife risk of Alzheimer's disease. Neuroscience; 2023 Feb. Available from: http://biorxiv.org/lookup/doi/10.1101/2023.01.31.526473.
23. Ying J, Keinath AT, Lavoie R, Vigneault E, El Mestikawy S, Brandon MP. Disruption of the grid cell network in a mouse model of early Alzheimer's disease. Nat Commun. 2022;13:886.
24. Koike R, Soeda Y, Kasai A, Fujioka Y, Ishigaki S, Yamanaka A, et al. Path integration deficits are associated with phosphorylated tau accumulation in the entorhinal cortex. Brain Communications. 2023;6:fcad359.
25. Shima S, Ohdake R, Mizutani Y, Tatebe H, Koike R, Kasai A, et al. Early detection of Alzheimer's disease pathophysiology using 3D virtual reality navigation: a correlational study with genetic and plasma biomarkers. 2024 [cited 2024 Jul 9]. Available from: http://medrxiv.org/lookup/doi/10.1101/2024.05.01.24306489.
26. Castegnaro A, Ji Z, Rudzka K, Chan D, Burgess N. Overestimation in angular path integration precedes Alzheimer's dementia. Curr Biol. 2023;33:4650-4661.e7.
27. Segen V, Ying J, Morgan E, Brandon M, Wolbers T. Path integration in normal aging and Alzheimer's disease. Trends Cogn Sci. 2022;26:142–58.
28. Folstein MF, Folstein SE, McHugh PR. Mini-mental state. J Psychiatr Res. 1975;12:189–98.
29. Akan O, Bierbrauer A, Kunz L, Gajewski PD, Getzmann S, Hengstler JG, et al. Chronic stress is associated with specific path integration deficits. Behav Brain Res. 2023;442: 114305.
30. Gérard T, Colmant L, Malotaux V, Salman Y, Huyghe L, Quenon L, et al. The spatial extent of tauopathy on [18F]MK-6240 tau PET shows stronger association with cognitive performances than the standard uptake value ratio in Alzheimer's disease. Eur J Nucl Med Mol Imaging. 2024;51:1662–74.
31. Malotaux V, Colmant L, Quenon L, Huyghe L, Gérard T, Dricot L, et al. Suspecting Non-Alzheimer's Pathologies and Mixed Pathologies: A Comparative Study Between Brain Metabolism and Tau Images. JAD. 2024;97:421–33.
32. Corder EH, Saunders AM, Strittmatter WJ, Schmechel DE, Gaskell PC, Small GW, et al. Gene Dose of Apolipoprotein E Type 4 Allele and the Risk of Alzheimer's Disease in Late Onset Families. Science. 1993;261:921–3.
33. Van der Linden M, Adam S, editors. L'évaluation des troubles de la mémoire: présentation de quatre tests de mémoire épisodique (avec leur étalonnage). Marseille: Solal; 2004.
34. De Partz M-P, Bilocq V, De Wilde V. Lexis: tests pour le diagnostic des troubles lexicaux chez le patient aphasique. Louvain-la-Neuve [Belgique]: De Boeck Solal; 2012.
35. Reitan RM. The relation of the Trail Making Test to organic brain damage. J Consult Psychol. 1955;19:393–4.
36. Rouleau I, Salmon DP, Butters N, Kennedy C, McGuire K. Quantitative and qualitative analyses of clock drawings in Alzheimer's and Huntington's disease. Brain Cogn. 1992;18:70–87.
37. Morris JC, Mohs RC, Rogers H, Fillenbaum G, Heyman A. Consortium to establish a registry for Alzheimer's disease (CERAD) clinical and neuropsychological assessment of Alzheimer's disease. Psychopharmacol Bull. 1988;24:641–52.
38. Ivanoiu A, Dricot L, Gilis N, Grandin C, Lhommel R, Quenon L, et al. Classification of Non-Demented Patients Attending a Memory Clinic using the New Diagnostic Criteria for Alzheimer's Disease with Disease-Related Biomarkers. JAD. 2014;43:835–47.
39. Desikan RS, Ségonne F, Fischl B, Quinn BT, Dickerson BC, Blacker D, et al. An automated labeling system for subdividing the human cerebral cortex on MRI scans into gyral based regions of interest. Neuroimage. 2006;31:968–80.
40. Fischl B, Salat DH, Busa E, Albert M, Dieterich M, Haselgrove C, et al. Whole Brain Segmentation. Neuron. 2002;33:341–55.
41. Greve DN, Salat DH, Bowen SL, Izquierdo-Garcia D, Schultz AP, Catana C, et al. Different partial volume correction methods lead to different conclusions: An 18F-FDG-PET study of aging. Neuroimage. 2016;132:334–43.
42. Greve DN, Svarer C, Fisher PM, Feng L, Hansen AE, Baare W, et al. Cortical surface-based analysis reduces bias and variance in kinetic modeling of brain PET data. Neuroimage. 2014;92:225–36.
43. Fischl B. FreeSurfer NeuroImage. 2012;62:774–81.
44. Bayart J-L, Hanseeuw B, Ivanoiu A, Van Pesch V. Analytical and clinical performances of the automated Lumipulse cerebrospinal fluid Aβ42 and T-Tau assays for Alzheimer's disease diagnosis. J Neurol. 2019;266:2304–11.
45. Hanseeuw BJ, Malotaux V, Dricot L, Quenon L, Sznajer Y, Cerman J, et al. Defining a Centiloid scale threshold predicting long-term progression to dementia in patients attending the memory clinic: an [18F] flutemetamol amyloid PET study. Eur J Nucl Med Mol Imaging. 2021;48:302–10.
46. Colmant L, Boyer E, Gerard T, Sleegers K, Lhommel R, Ivanoiu A, et al. Definition of a Threshold for the Plasma Aβ42/Aβ40 Ratio Measured by Single-Molecule Array to Predict the Amyloid Status of Individuals without Dementia. IJMS. 2024;25:1173.
47. Bates D, Mächler M, Bolker B, Walker S. Fitting Linear Mixed-Effects Models using lme4. arXiv; 2014 [cited 2022 Sep 12]. Available from: http://arxiv.org/abs/1406.5823.
48. Russell, Lenth. emmeans: estimated Marginal Means, aka Least-Squares Means. R package version 1.4. 3.01. The University of Iowa Iowa City, IA; 2019.
49. Mokrisova I, Laczo J, Andel R, Gazova I, Vyhnalek M, Nedelska Z, et al. Real-space path integration is impaired in Alzheimer's disease and mild cognitive impairment. Behav Brain Res. 2016;307:150–8.
50. Hill PF, Bermudez S, McAvan AS, Garren JD, Grilli MD, Barnes CA, et al. Age differences in spatial memory are mitigated during naturalistic navigation. Aging Neuropsychol Cogn. 2024;31:1106–30.
51. Hanseeuw BJ, Betensky RA, Jacobs HIL, Schultz AP, Sepulcre J, Becker JA, et al. Association of Amyloid and Tau With Cognition in Preclinical Alzheimer Disease: A Longitudinal Study. JAMA Neurol. 2019;76:915.
52. Nelson PT, Alafuzoff I, Bigio EH, Bouras C, Braak H, Cairns NJ, et al. Correlation of Alzheimer Disease Neuropathologic Changes With Cognitive Status: A Review of the Literature. J Neuropathol Exp Neurol. 2012;71:362–81.
53. Bhasin G, Calvin-Dunn KN, Hyman JM. Spatial navigation: Alzheimer's pathology disrupts movement-based navigation. Curr Biol. 2023;33:R688-91.
54. Coughlan G, DeSouza B, Zhukovsky P, Hornberger M, Grady C, Buckley RF. Spatial cognition is associated with levels of phosphorylated-tau and β-amyloid in clinically normal older adults. Neurobiol Aging. 2023;130:124–34.
55. Worsley C. Path integration following temporal lobectomy in humans. Neuropsychologia. 2001;39:452–64.
56. Stemmler M, Mathis A, Herz AVM. Connecting multiple spatial scales to decode the population activity of grid cells. Sci Adv. 2015;1: e1500816.
57. Evans T, Bicanski A, Bush D, Burgess N. How environment and self-motion combine in neural representations of space: Environment and self-motion in neural representations of space. J Physiol. 2016;594:6535–46.
58. Winter SS, Clark BJ, Taube JS. Disruption of the head direction cell network impairs the parahippocampal grid cell signal. Science. 2015;347:870–4.
59. Mahmood O, Adamo D, Briceno E, Moffat SD. Age differences in visual path integration. Behav Brain Res. 2009;205:88–95.
60. Adamo DE, Briceño EM, Sindone JA, Alexander NB, Moffat SD. Age differences in virtual environment and real world path integration. Front Ag Neurosci. 2012 [cited 2022 Sep 20];4. Available from: http://journal.frontiersin.org/article/10.3389/fnagi.2012.00026/abstract.
61. Harris MA, Wolbers T. Ageing effects on path integration and landmark navigation. Hippocampus. 2012;22:1770–80.
62. Stangl M, Kanitscheider I, Riemer M, Fiete I, Wolbers T. Sources of path integration error in young and aging humans. Nat Commun. 2020;11:2626.

63. Lich M, Bremmer F. Self-motion perception in the elderly. Front Hum Neurosci. 2014 [cited 2022 Sep 27];8. Available from: http://journal.frontiersin.org/article/10.3389/fnhum.2014.00681/abstract.
64. Zhong JY. Neuroscience research on human visual path integration: Topical review of the path completion paradigm and underlying role of the hippocampal formation from a strategic perspective. Behav Neurosci. 2022;136:503–27.
65. O'Keefe JM, Nadel L, O'Keefe J. The hippocampus as a cognitive map. Oxford: Clarendon Press; 1978.
66. Hanseeuw BJ, Jacobs HIL, Schultz AP, Buckley RF, Farrell ME, Guehl NJ, et al. Association of Pathologic and Volumetric Biomarker Changes With Cognitive Decline in Clinically Normal Adults: Harvard Aging Brain Study. Neurology. 2023 [cited 2024 Dec 24];101. Available from: https://www.neurology.org/doi/10.1212/WNL.0000000000207962.

Publisher's Note